

Technical note

A versatile shear and compression apparatus for mechanical stimulation of tissue culture explants

Eliot H. Frank^{a,*}, Moonsoo Jin^a, Andreas M. Loening^a, Marc E. Levenston^b, Alan J. Grodzinsky^a

^a*Continuum Electromechanics Group, Center for Biomedical Engineering, Department of Electrical Engineering and Computer Science, Massachusetts Institute of Technology, Room 38–377, Cambridge, MA 02139, USA*

^b*Department of Mechanical Engineering, Georgia Institute of Technology, Atlanta, GA USA*

Accepted 14 April 2000

Abstract

We have developed an incubator housed, biaxial-tissue-loading device capable of applying axial deformations as small as 1 μm and sinusoidal rotations as small as 0.01° . Axial resolution is 50 nm for applying sinewaves as low as 10 μm (or 1% based on a 1 mm thickness) or as large as 100 μm . Rotational resolution is 0.0005° . The machine is small enough (30 cm high \times 25 cm \times 20 cm) to be placed in a standard incubator for long-term tissue culture loading studies. In metabolic studies described here, application of sinusoidal macroscopic shear deformation to articular cartilage explants resulted in a significant increase in the synthesis of proteoglycan and proteins (uptake of ^{35}S -sulfate and ^3H -proline) over controls held at the same static offset compression. © 2000 Elsevier Science Ltd. All rights reserved.

Keywords: Mechanotransduction; Shear; Tissue loading; Chondrocyte metabolism; Cartilage biomechanics

1. Introduction

Joint loading *in vivo* results in a complex combination of compressive, tensile, and shear deformations in cartilage. Mechanical loading plays a crucial role in the development and maintenance of normal articular cartilage. Various loading-induced physical phenomena (fluid pressure, cell/matrix deformation, streaming potential, etc.) have been proposed to play different roles in metabolic regulation (Giori et al., 1993; Grodzinsky et al., 1998). Several *in vitro* studies of physical regulation of cartilage metabolism have utilized various mechanical stimuli such as dynamic compression (Sah et al., 1989; Bonassar et al., 1998), cyclic hydrostatic pressure (Hall et al., 1991), and fluid-induced shear stress (Smith et al., 1995). Dynamic compression is particularly complex, inducing volumetric changes, shear stresses, and gradients in intratissue pressure and fluid flow, which have been spatially associated with metabolic stimulation

(Kim et al., 1994). In contrast, macroscopic shear deformation of a poroelastic tissue such as articular cartilage should not induce volumetric changes, intratissue fluid flow or pressure gradients. While investigators have examined fluid-induced shear stress in monolayer cell culture (Smith et al., 1995; Yellowley et al., 1997), we do not know of any studies of the effects of macroscopic shear deformation of tissue explants on chondrocyte metabolism.

Previous studies indicate that fluid flow and/or fluid pressure gradients are capable of stimulating articular cartilage metabolism, but the stimulatory potential of macroscopic matrix shear (without associated fluid flow) is unknown. The ability to apply direct shear to explants, as well as compression, could help separate the role of intratissue fluid flow and hydrostatic pressure gradients from matrix and cell deformation (without fluid flow) as potential mediators of cell metabolism. To compare and contrast with previous work using cyclic axial compression, our objectives were: (1) to develop a biaxial system capable of applying both large and small cyclic shear and compression to articular cartilage explants in tissue culture and (2) to study the biosynthetic response of chondrocytes to dynamic tissue macroscopic shear deformation.

* Corresponding author. Tel.: + 1-617-253-4969; fax: + 1-617-258-5239.

E-mail address: ehfrank@mit.edu (E.H. Frank).

2. Methods

2.1. Shear/compression apparatus

A rigid frame (30 cm high \times 25 cm \times 20 cm) was constructed consisting of two 0.95 cm thick top and bottom stainless-steel plates bolted to three 2.54 cm diameter stainless-steel rods (Fig. 1). A third stainless-steel plate was clamped to the support rods to allow repositioning for different experimental shear or compression chambers. A linear stepper motor (23A-6102A, American Precision, Buffalo, NY) mounted to the top plate has a threaded rotor which engages a threaded rod. The threaded rod in turn is attached to a carriage plate and a pair of linear bearings which ride on two of the support rods. The axial motor is capable of applying compressive ramps at rates up to 1 mm/s with an applied force up to 400 N. The rotational fixture consists of a rotary position table (6R180, Design Components, Franklin, MA) with a 180:1 gear reduction ratio driven by a conventional stepper motor (23D-6306, American Precision). A block placed at 6.35 cm from the center of the rotating table contacts an LVDT to measure angular displacement. For small angular rotations, the displacement of the block sensed by the LVDT is essentially a linear function of angular rotation.

Each motor is driven by a micro-stepper drive (IM483, Intelligent Motion Systems, Marlborough, CT). The drives are electrically isolated via internal opto-couplers and each have their own power supply separate from the analog and digital electronics power supply. The micro-stepper drives combined with the motors and gearing provide a theoretical axial resolution of 50 nm and rotational resolution of 0.0005°. Both axial and angular displacements are measured by linear variable differential transformers (LVDT, Model S5, Sensotec, Columbus, OH). Various load transducers (10, 100, and 500 N capacities, Model 31, Sensotec) and/or torque transducers (5 N m capacity, Transducer Techniques, Temecula, CA, or 0.2 N m capacity, QWLC-8M, Sensotec) may be rigidly attached in series between the carriage and sample chamber lid (Fig. 1) to measure compressive and shear stress in the samples. Rotational control is integrated with axial control so that shear tests may be intermixed with compression tests in the same experimental procedure.

2.2. Control and data acquisition

The control electronics, including the transducer-signal conditioners for the LVDTs, load cells, and torque cells as well as the limit, feedback, and digital switching circuits were mounted on two prototype circuit boards with copper cladding acting as a ground plane. A digitally-controlled analog switch allows any one of the axial displacement, angular displacement, axial load,

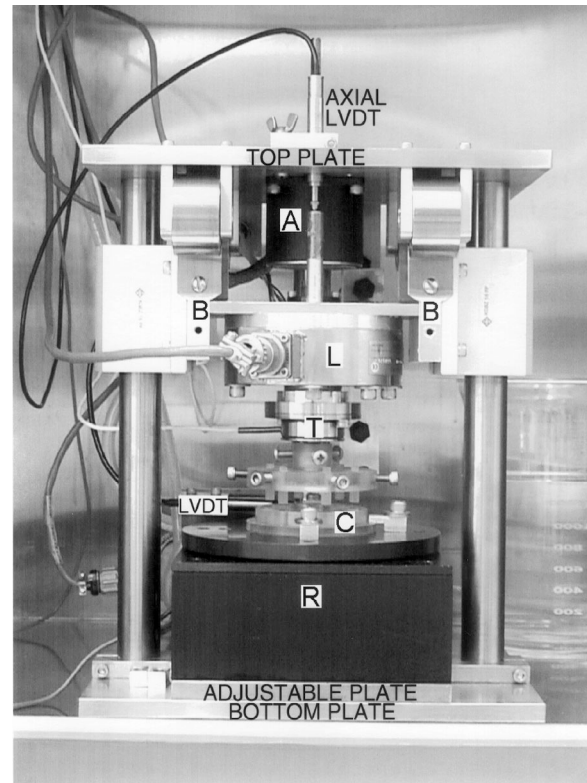


Fig. 1. Shear/compression apparatus: A — axial linear stepper motor; B — bearing/carriage assembly; C — sample chamber; L — load cell; T — torque cell; R — rotary position table. The adjustable plate may be moved to accommodate other fixtures. The LVDT shown to left of chamber (C) senses rotational displacement. Rotary table (R) is driven by stepper motor behind the table.

or torque signals to be used for closed-loop feedback control. A computer-based data acquisition system provides control and monitoring of the apparatus. The data acquisition and control subsystem consists of a multi-function I/O card (AT-MIO-16DL-9, National Instruments, Austin, TX), which provides high-speed analog-to-digital conversion (ADC) and digital I/O, and a 10-channel digital-to-analog converter (DAC) board (AT-AO-10, National Instruments). The DAC channels provide signal offsets as well as ramp and sinewave control signals. In axial displacement feedback control, sinusoid waveform distortion is less than 1% for a 10 μ m amplitude sinewave, comparable to that of our Dynastat mechanical spectrometer (Dynastatics, Albany, NY) (\sim 0.3%) which we have used in our previous studies on cartilage metabolic response to dynamic compression (Sah et al., 1989).

2.3. Explant studies

Cartilage disks (3 mm diameter, 1.1 mm thick) were obtained from the femoropatellar groove of 1–2 week old calves using established methods (Sah et al., 1989). and

maintained in culture media (low-glucose DMEM with 10 mM Hepes, 10% (v/v) FBS, 0.1 mM nonessential amino acids, an additional 0.4 mM proline, and 20 $\mu\text{g/ml}$ ascorbate). Up to 12 cartilage explants were placed in individual media-filled wells of a polysulphone chamber (Fig. 2) fixed to the rotary positioning table and compressed (radially unconfinned) by a non-rotating polysulphone lid.

2.4. Mechanical tests

Matched cartilage disks from a single anatomical site (4 at a time) were subjected to cyclic shear deformation (0.01–1 Hz) at nominal engineering shear strains of 0.4–1.6%. (These amplitudes and frequencies were chosen to correspond to the values of interest in the shear metabolic studies reported below, and are similar to the ranges of frequency and strain used in previous *in vitro* compressive metabolic studies.) As the 12 wells are arranged in a circle, the average engineering shear strain in the samples is computed as the rotation angle (θ) times the circle radius (R) divided by sample thickness (h)

$$\gamma = \theta R/h. \quad (1)$$

Since the explants are located far ($R = 25.4$ mm) from the rotational axis, rotation of the chamber base applies a nearly uniform simple shear deformation to the cartilage disks ($100 \pm 6\%$ of nominal value across the plug diameter). In this configuration, the apparatus can apply sinusoidal shear strains on a 1 mm thick sample as small as 0.5% in feedback control (with $\sim 1\%$ distortion, Fig. 3) and as large as 4%, as well as ramps up to 40% shear strain. The average dynamic shear stress applied to the samples was computed from the recorded torque ($n = 4$ sets of 4 disks) as

$$\tau = T/(RA) \quad (2)$$

where T is the measured torque amplitude and A is the total sample area of all the disks. Finally, the effective shear modulus (Fung, 1965), G , of the cartilage disks was computed as

$$G = \tau/\gamma. \quad (3)$$

For analysis of sinusoidal signals, θ , γ , T , and τ represent amplitudes of angle, shear strain, torque, and shear stress waveforms, respectively, and G is the magnitude of the complex shear modulus (Ward, 1965).

2.5. Metabolic studies

In one series of tests, anatomically matched disks were randomly assigned to dynamic shear, statically compressed control, and free-swelling groups ($N = 18$). Using a lid with 6 platens, experimental disks (6 at a time) were slowly compressed to a thickness of 1 mm. After equilibrium was obtained, the disks were subjected to continuous

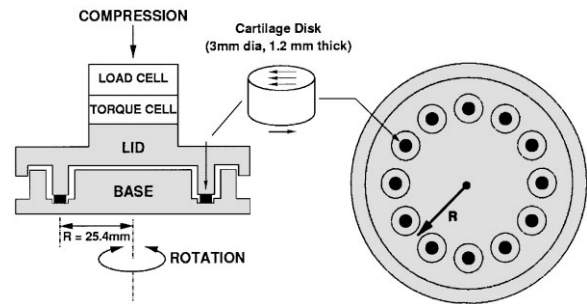


Fig. 2. Cartilage explants are placed in wells in the base of an autoclavable polysulphone chamber, similar in design to those previously used for static compression experiments (Quinn et al., 1998). The platens of the nonrotating lid compress the cartilage. The platen surfaces were roughened, but no adhesives were used in culture experiments involving shear deformation. For some tests, a lid with only 6 platens was used so that 6 out of 12 plugs were loaded while another 6 plugs in the alternate wells were unloaded controls.

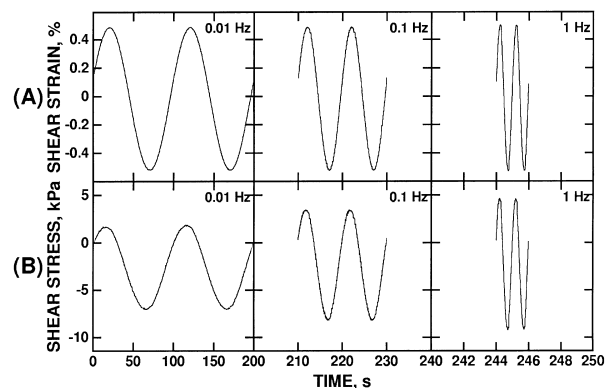


Fig. 3. Examples of (A) applied sinusoidal shear strain, and (B) resulting stress waveforms at 0.01, 0.1 and 1 Hz for 4 articular cartilage disks tested simultaneously in the chamber of Fig. 2 (spaced symmetrically at 90° apart). The time axis is expanded in middle and right panels to show details. Shear stress waveform indicates an increase in shear modulus with frequency. The phase angle of stress relative to strain was approximately 10° at all 3 frequencies.

dynamic shear deformation (nominally 1%) at 0.1 Hz for 24 h. In separate tests, matched control disks were also compressed to 1 mm in the same chamber and held for 24 h with no dynamic shear deformation. During each dynamic or static test, 6 matched free-swelling control disks were maintained with no applied loading in the 6 wells of the chamber that did not have loading platens. During the entire 24-h loading period, disks were incubated with 10 $\mu\text{Ci/ml}$ ^{35}S -sulfate and 20 $\mu\text{Ci/ml}$ ^3H -proline as measures of proteoglycan and total protein synthesis.

2.6. Spatial localization of biosynthesis

In two separate experiments, cartilage disks were subjected to 0.1 Hz, 1% shear deformation for 12 h, and a 2 mm diameter core was removed from each 3 mm dynamic and static control disk; ^{35}S -sulfate incorporation

was analyzed separately in the 2 mm diameter core and in the remaining annular ring (Kim et al., 1994).

2.7. Statistics

Groups were compared using paired and unpaired *t*-tests with a significance level of $p < 0.05$.

3. Results

3.1. Mechanical tests

At 10% axial offset strain and shear strains $\leq 1\%$, the dynamic shear modulus was in the range of 0.6–1.5 MPa consistent with values for articular cartilage reported previously (Spirt et al., 1989; Zhu et al., 1993). The dynamic shear modulus increased with frequency (Fig. 3) and compressive offset strain (data not shown). The magnitude of the apparent shear modulus also decreased with increasing shear strain. At strains in excess of 1.2%, the torque waveforms showed distortion indicative of slipping between the tissue and the platens.

3.2. Metabolic effects

Both ^{35}S -sulfate and ^3H -proline incorporation in dynamically sheared disks at 0.1 Hz and 1% applied shear strain were significantly higher ($p < 0.002$) by 25 and 41%, respectively, than in control disks held at the same static offset compression (Fig. 4). Unloaded free-swelling controls placed in adjacent wells of the chamber showed incorporation rates of ^{35}S -sulfate (42 ± 16 pmol/ μg DNA/h) and ^3H -proline (82 ± 23 pmol/ μg DNA/h) that were comparable to previous results (Sah et al., 1989) and not significantly different from statically compressed controls (Fig. 4).

The two experiments ($N = 6$ disks, $N = 5$ disks) involving spatial localization of proteoglycan synthesis were performed and analyzed in a manner identical to that of Kim et al., 1994, but using shear rather than axial compression. The sulfate incorporation rates per μg DNA in the 2 mm cores and annular rings of dynamically sheared disks were normalized to the average incorporation rates of the static control disks. The normalized rates in the dynamically sheared cores and rings were pooled ($N = 11$); there was no significant difference between the normalized sulfate incorporation rates in the 2 mm core and annular ring of the dynamically sheared samples ($p > 0.28$, power > 0.95).

4. Discussion

We have previously reported using an incubator-housed compression system to study the effects of axial

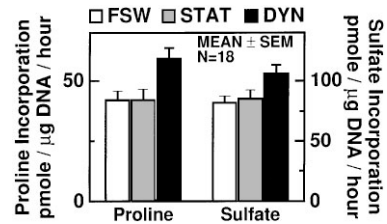


Fig. 4. ^{35}S -sulfate and ^3H -proline incorporation in free-swelling controls (FSW, open bars), statically compressed (STAT, shaded bars), and dynamically sheared (DYN, solid bars, 0.1 Hz, 1% shear strain) disks. Incorporation in dynamically sheared disks was significantly higher ($p < 0.002$) than in free-swelling or static control disks.

dynamic compression on the response of cartilage to IGF-1 (Bonassar et al., 1998), and on the effects of dynamic compression on biosynthesis by chondrocytes seeded into alginate gel disks (Ragan et al., 1998). The new biaxial loading apparatus described here has performed well in an incubator environment, accurately applying desired compressive or shear strains to cartilage explants. We have been able to perform both material property testing in addition to metabolic studies of tissue in shear and compression in a sterile incubator environment. Shear modulus tests have been performed in our apparatus in both torsional (pure shear) and simple shear modes on similar cartilage disks to validate our measurement methodology. The control software allows axial or rotational ramps and sinusoids of various amplitudes to be intermixed and repeated according to any desired protocol.

The biomechanical properties of articular cartilage explants tested in simple shear agreed well with previously reported viscoelastic shear properties of articular cartilage tested in simple shear (Spirt et al., 1989) and pure shear (Zhu et al., 1993), demonstrating an increased dynamic stiffness with increased frequency and compressive offset strain. The softening effect we observed with increasing strain amplitude is in agreement with previous reports of nonlinear viscoelastic behavior in cartilage (Simon et al., 1990) and meniscus (Zhu et al., 1994). Comparable shear moduli (values within 10–20%) and softening effects were observed in separate low strain torsional (pure shear) tests of individual 8.4 mm diameter cartilage disks using the same apparatus (Jin, 1999) and in verification experiments in which sand-paper was glued to the loading platens. At shear strains greater than 1.2% in mechanical tests, we noted distorted torque waveforms indicative of slipping.

In the metabolic studies, 0.1 Hz dynamic shear deformation produced significant increases in synthesis of proteoglycans and proteins. Unlike pure shear deformation, small amplitude simple shear deformation (Love, 1944) may induce low levels of fluid flow localized near the leading and trailing edges of the explants (due to

bending-induced pressure gradients). As fluid flow has been associated with metabolic stimulation in dynamic unconfined compression studies (Kim et al., 1994) and fluid induced shear of chondrocytes in monolayer (Smith et al., 1995), this raises the possibility of local stimulation by fluid flow near the outer edge of the disks subjected to simple shear. In our experiments, however, fluid velocities resulting from macroscopic matrix shear deformation are substantially lower than that in axially compressed disks (Kim et al., 1994), and many orders of magnitude lower than that in monolayer studies (Smith et al., 1995). Finite element model simulations of cartilage mechanical response (Levenston et al., 1998) indicate that fluid flow and fluid pressure gradients in response to dynamic simple shear are confined to the edges, but with amplitudes that are less than 1% of those induced by axial compression (at equal axial compression and shear strain amplitudes). The fact that both the core region (with no fluid flow) and outer annular region of the explants showed comparable metabolic stimulation in response to matrix shear (in contrast to significant ring vs. core differences found by Kim et al. (1994) for axial compression) suggests that matrix shear deformation and not fluid flow, is responsible for the metabolic stimulation seen in the data of Fig. 4. Ongoing studies are examining effects of a range of shear strain amplitudes and frequencies, as well as differences in gene expression under dynamic shear deformation.

Acknowledgements

This work was supported by NIH Grants AR33236 and AR45779 and an Arthritis Foundation Postdoctoral Fellowship to M.E. Levenston.

References

- Bonassar, L.J., Grodzinsky, A.J., Davila, S.G., Trippel, S.B., 1998. The effects of dynamic compression on the response of cartilage to IGF-1. In: Transactions of the Orthopaedic Research Society, New Orleans, LA, Vol. 23, p. 579.
- Fung, Y.C., 1965. Foundations of Solid Mechanics.. Prentice-Hall, Englewood Cliffs, NJ.
- Giori, N.J., Beaupré, G.S., Carter, D.R., 1993. Cellular shape and pressure may mediate mechanical control of tissue composition in tendons. *Journal of Orthopaedic Research* 11, 581–591.
- Grodzinsky, A.J., Kim, Y.J., Buschmann, M.D., Quinn, T.M., Garcia, A.M., Huziker, E.B., 1998. Response of the chondrocyte to mechanical stimuli. In: Brandt, K.D., Doherty, M., Lohmander, L.S. (Eds.), *Osteoarthritis*. Oxford University Press, Oxford, pp. 123–136.
- Hall, A.C., Urban, J.P.G., Gehl, K.A., 1991. The effects of hydrostatic pressure on matrix synthesis in articular cartilage.. *Journal of Orthopaedic Research* 9, 1–10.
- Jin, M., 1999. Regulation of cartilage metabolism by dynamic tissue shear strain and the mechanical characterization of cartilage. Master's Thesis, Massachusetts Institute of Technology, Cambridge, MA.
- Kim, Y.-J., Sah, R.L.-Y., Grodzinsky, A.J., Plaas, A.H.K., Sandy, J.D., 1994. Mechanical regulation of cartilage biosynthetic behavior: physical stimuli. *Archives of Biochemistry and Biophysics* 311, 1–12.
- Levenston, M.E., Frank, E.H., Grodzinsky, A.J., 1998. Variationally derived 3-field finite element formulations for quasistatic poroelastic analysis of hydrated biological tissues. *Computational Methods of Applied Mechanics and Engineering* 156, 231–246.
- Love, A.E.H., 1944. *A Treatise on the Mathematical Theory of Elasticity*.. Dover, New York.
- Quinn, T.M., Grodzinsky, A.J., Buschmann, M.D., Kim, Y.-J., Huziker, E.B., 1998. Mechanical compression alters proteoglycan deposition and matrix deformation around individual cells in cartilage explants. *Journal of Cell Science* 111, 573–583.
- Ragan, P.M., Staples, A.K., Hung, H.K., Chin, V.I., Binette, F., Grodzinsky, A.J., 1998. Mechanical compression influences chondrocyte metabolism in a new alginate disk culture system. In: Transactions of the Orthopaedic Research Society, New Orleans, LA, Vol. 12, p. 991.
- Sah, R.L., Kim, Y.-J., Doong, J.H., Grodzinsky, A.J., Plaas, A.H.K., Sandy, J.D., 1989. Biosynthetic response of cartilage explants to dynamic compression. *Journal of Orthopaedic Research* 7, 619–636.
- Simon, W.H., Mak, A., Spirt, A., 1990. The effect of shear fatigue on bovine articular cartilage. *Journal of Orthopaedic Research* 8, 86–93.
- Smith, R.L., Donlon, B.S., Gupta, M.K., Mohtai, M., Das, P., Carter, D.R., Cooke, J., Gibbons, G., Hutchinson, N., Schurman, D.J., 1995. Effects of fluid-induced shear on articular chondrocytes morphology and metabolism in vitro. *Journal of Orthopaedic Research* 13, 824–831.
- Spirt, A.A., Mak, A.F., Wassell, R.P., 1989. Nonlinear viscoelastic properties of articular cartilage in shear. *Journal of Orthopaedic Research* 7 (1), 43–49.
- Ward, I.M., 1965. *Mechanical Properties of Solid Polymers*.. Wiley-Interscience, New York.
- Yellowley, C.E., Jacobs, C.R., Li, Z., Zhou, Z., Donahue, H.J., 1997. Effects of fluid flow on intracellular calcium in bovine articular chondrocytes. *American Journal of Physiology* 273, C30–C36.
- Zhu, W., Mow, V.C., Koob, T.J., Eyre, D.R., 1993. Viscoelastic shear properties of articular cartilage and the effects of glycosidase treatments. *Journal of Orthopaedic Research* 11, 771–781.
- Zhu, W., Chern, K.Y., Mow, V.C., 1994. Anisotropic viscoelastic shear properties of bovine meniscus. *Clinical Orthopaedics* 306, 34–45.